Charged and neutral exciton complexes in individual self-assembled In(Ga)As quantum dots

J. J. Finley,[1] A. D. Ashmore,[1] A. Lemaître,[1] D. J. Mowbray,[1] M. S. Skolnick,[1] I. E. Itskevich,[2] P. A. Maksym,[3] M. Hopkinson,[4] and T. F. Krauss[5]

[1]*Department of Physics and Astronomy, University of Sheffield, Sheffield S3 7RH, United Kingdom*

[2]*The School of Engineering, University of Hull, Kingston upon Hull HU6 7RX, United Kingdom*

[3]*Department of Physics and Astronomy, University of Leicester, University Road, Leicester LE1 7RH, United Kingdom*

[4]*Department of Electronic and Electrical Engineering, University of Sheffield, Sheffield S1 3JD, United Kingdom*

[5]*Department of Physics and Astronomy, University of St. Andrews, North Haugh, St. Andrews, Fife KY16 9SS, United Kingdom*

(Received 7 August 2000; published 29 January 2001)

Charged (X^*) and neutral (X) exciton recombination is reported in the photoluminescence spectra of single In(Ga)As quantum dots. Photoluminescence excitation (PLE) spectra show that the charged excitons are created only for excitation in the barrier or cladding layers of the structure, consistent with their charged character, whereas the neutral excitons in addition show well-defined excitation features for resonant excitation of the dots. The PLE spectra for X and X^* exhibit a clear anticorrelation in the region of the wetting layer transition, showing that they compete for photocreated carriers.

DOI: 10.1103/PhysRevB.63.073307 PACS number(s): 73.21.−b, 71.35.−y, 85.35.Be

In recent years, self-assembled semiconductor quantum dots (SAQD's) have developed into one of the most topical fields in nanostructure research.[1] This interest is driven both by the potential for high-performance device applications[1,2] and the possibility to investigate novel physical phenomena in a quasi-zero-dimensional (0D) system. Of particular interest from a fundamental viewpoint are the modifications of the optical properties predicted to arise from Coulomb interaction and correlation effects. Detailed calculations have shown that the form of the excitonic spectrum is strongly dependent upon the number and configuration of electrons and holes[3–6] and the charge status (excess electrons or holes)[7] of the dots.

The influence of excess electron occupation on the optical properties of SAQD's has been reported for large ensembles using conventional spectroscopic techniques.[8,9] Detailed interpretation is, however, complicated by inhomogeneous broadening (>30 meV), which obscures Coulomb effects involving energy shifts at the ~meV level. More recently, the development of spatially resolved techniques has circumvented these problems, enabling the investigation of individual dots for which the broadening is purely homogeneous (<50 μeV). Using such techniques, the effects of Coulomb interactions in charged neutral dots[10–15] has been reported, with two works appearing very recently on charged 0D systems controlled either by doping[16] or electrostatically.[17]

Most descriptions of the carrier population kinetics of SAQD's assume capture of correlated electron-hole pairs into the dots from an external reservoir (barrier material or wetting layer) with a steady-state occupation governed by the relative time scales for carrier capture (electrons plus holes in equal numbers), relaxation, and radiative recombination.[1,18,19] In this case, the Coulomb interactions involve charge neutral excitons[10–15] resulting in the sequential appearance of lines in the ground-state (s-shell) emission, with increasing exciton occupation, arising from single exciton (X), biexciton ($2X$), and higher-order complexes ($3X$,$4X$,...). However, electrons and holes may be separately captured into the dot and both charged and neutral excitonic species are likely to arise in the time-averaged emission spectrum.

In this work, we use microphotoluminescence (μPL) spectroscopy to investigate charged *and* neutral exciton complexes in individual In(Ga)As SAQD's incorporated into a graded gap double heterostructure. We show that the charge status of the most prominent excitonic species observed depends on the photon energy of the excitation, with very different PL excitation (PLE) spectra being found for the charged and neutral species. Accurate power-dependent measurements are used to identify the number of excitons in the dot for single- and few-exciton emission lines.

The samples investigated were grown using molecular-beam epitaxy (MBE) on a [100]-orientated n^+ GaAs substrate. Following a 300-nm-thick GaAs buffer, the layer sequence was 1350-nm-thick $Al_{0.33}Ga_{0.66}As$ blocking barrier followed by a 175-nm $Al_{0.13}Ga_{0.87}As$ cladding layer and 25-nm GaAs. The QD layer was then deposited, consisting of 2.4 monolayers (ML) of InAs grown at 500 °C at 0.01 ML sec, producing SAQD's with dimensions $\sim 18\times 18\times 5$ nm and areal density $\sim 10^{10}\,cm^{-2}$. The structure was completed with 25-nm GaAs and a second 175-nm-thick $Al_{0.13}Ga_{0.87}As$ cladding layer. The resulting conduction and valence band-edge profile is shown in Fig. 1(a). After growth, the sample was rapidly thermally annealed (300 s at 750 °C) to blueshift the low-temperature QD emission[20] to ~1330 meV, where it is accessible to sensitive Si-based detectors. Following annealing, the wetting layer emission was observed at $E_{WL} = 1460 \pm 5$ meV (1420 meV before annealing). To isolate individual QD's for investigation, the annealed material was then fabricated into an array of widely spaced ~100 and ~200-nm-diam mesas using e-beam lithography and plasma etching. Only mesas that exhibited a single emission line under low excitation density ($P_{ex} \sim 1\,W\,cm^{-2}$), indicative of a single optically active QD, were chosen for further investigation. μPL was performed at $T \sim 10$ K on these mesas using a microscope objective (numerical aperture~0.6) to provide a submicron excitation spot, accurately positioned (± 0.05 μm) on the sample using piezoactuators. PL was excited using a Ti-sapphire laser tuneable from 1350–1550 meV. PL was collected via the same objective, dispersed

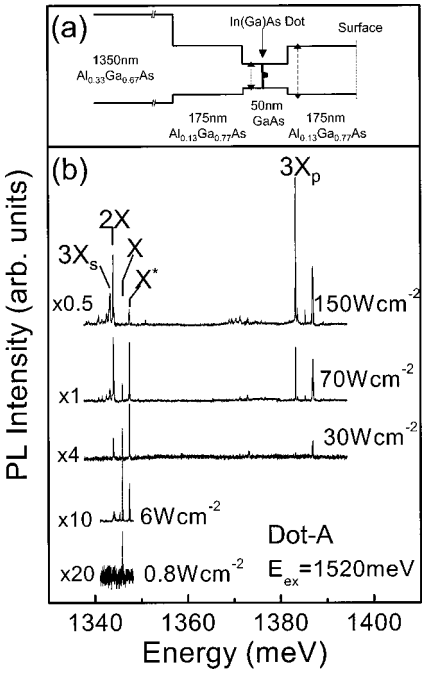

FIG. 1. (a) Band-edge profile of the structure. The dotted and dashed vertical lines indicate 1520- and 1730-meV excitation, respectively. (b) Low-temperature ($T=10$ K) PL spectra, for excitation energy of 1520 meV as a function of power density (0.8–150 W cm^{-2}) for a single self-assembled quantum dot (dot-*A*). The emission features around ~1340 meV arise from *s*-shell single- and few-exciton recombination while the peaks close to ~1385 meV arise from *p*-shell recombination.

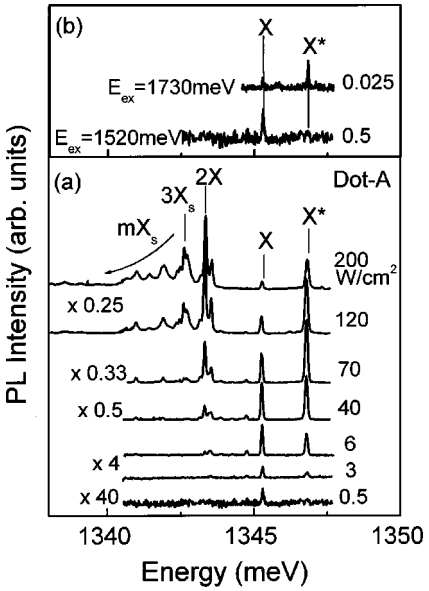

FIG. 2. (a) *s*-shell PL spectra from dot-*A* as a function of excitation intensity. (b) PL spectra from dot-*A* using global (1730 meV) and local (1520 meV) excitation energies.

using a 0.85-m double monochromator (resolution ~25 μeV), and detected by either a CCD camera or Si-avalanche photodiode.

PL spectra from a single dot (dot-*A*) are presented in Fig. 1(b) as a function of $P_{\rm ex}$ (occupancy $\tilde{N}_X$) for an excitation energy of 1520 meV at the GaAs band edge [the dashed line in Fig. 1(a)]. The ground-state (*s*-shell) emission is shown on an expanded scale in Fig. 2(a). At the lowest excitation levels investigated, a single narrow (full width at half maximum <40 μeV, resolution-limited) emission line, labeled X [Figs. 1(b) and 2(a)], is observed at 1345.3 meV, shown later to arise from single neutral exciton recombination (X). For higher $P_{\rm ex}$, the complexity of the spectrum increases with two additional lines (X^* and $2X$) appearing, separated from X by $+1.5\pm0.1$ and -2 ± 0.1 meV, respectively, identified later as single charged exciton (X^*) and neutral biexciton ($2X$) recombination, respectively.

Concomitant with the first appearance of $2X$, excited-state (*p*-shell) emission is seen 35–45 meV to higher energy (around 1385 meV), observed when relaxation to the ground state is blocked by an exciton of the same spin. For higher $P_{\rm ex}$, additional features (mX_s [Fig. 2(a)]), appear on the low-energy side of $2X$, and become increasingly dominant at higher $P_{\rm ex}$. These features arise from multiexciton ($m\geqslant3$) recombination and span an energy band 5–7 meV below X. Each line arises from recombination of an *s*-shell exciton, perturbed by the presence of excitons occupying higher-lying (p,d) states.[3,15] The larger width of the mX_s lines, relative to X, may arise from the greater multiplicity of initial- and final-state configurations or possibly lifetime broadening since the final state[3] containing a *p*-shell exciton is not a ground state of the system.

To establish unambiguously the exciton occupancy for X, X^*, $2X$, and $3X_s$, power-dependent measurements were performed using a continuously graded neutral density filter and single photon-counting setup. The integrated emission intensities (I_X, I_{X^*}, I_{2X}, and I_{3X_s}) for $E_{\rm ex}=1520$ meV are presented in Fig. 3 on log-linear (a) and log-log (b) scales. All results are background-corrected. The results in Fig. 3 are for a second single dot (dot-*B*), which exhibits very similar spectra to those in Figs. 1 and 2 but is shifted by ~15 meV to higher energy (Fig. 3, inset). The form of the power dependences from the two dots was also very similar. Nearly identical spectra were found for five more dots, demonstrating that the detailed form of the *s*-shell PL is determined by *intrinsic* effects, and not, for example, from perturbations due to ionized impurities or processing-induced defects.

Figure 3(b) shows that *both* I_X and I_{X^*} increase linearly with excitation power (exponent $m_{X/X^*}=1.05\pm1$) before simultaneously reaching a maximum at ~400 W cm^{-2} and decreasing to higher energy. This behavior confirms that both X and X^* arise from *single*-exciton occupancy of the dot. In addition, I_{2X} increases quadratically in Fig. 3(b) with $P_{\rm ex}$ ($m=1.9\pm0.1$) confirming its identification as biexciton recombination. The X and X^* lines do not exhibit any linear polarization and thus it can be concluded with certainty that they do not arise from splitting due to an asymmetric lateral confinement potential. In addition, the close similarity in the I_X and I_{X^*} behavior in Fig. 3 indicates that the exciton capture kinetics for both X and X^* formation are similar, both complexes being formed by barrier band-edge excitation of the system. We demonstrate below that X^* is only excited by photocreating *e-h* pairs *outside* the dot, in the barrier mate-

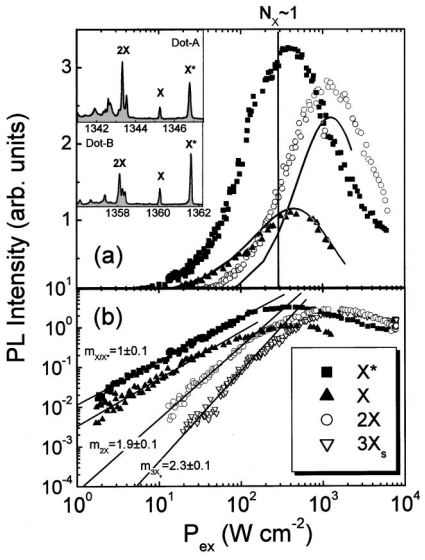

FIG. 3. Detailed intensity variation of X, X^*, and $2X$ for dot-B as a function of excitation density on log-linear and log-log scales in (a) and (b), respectively. The exponents of X and X^* in (a) are very close to unity below 100 W cm^{-2}, confirming their single-exciton origin. For $2X$ the exponent is 1.9 ± 0.1, supporting its biexciton attribution. Inset: Comparison of s-shell emission from dots A and B demonstrating the generality of the spectra.

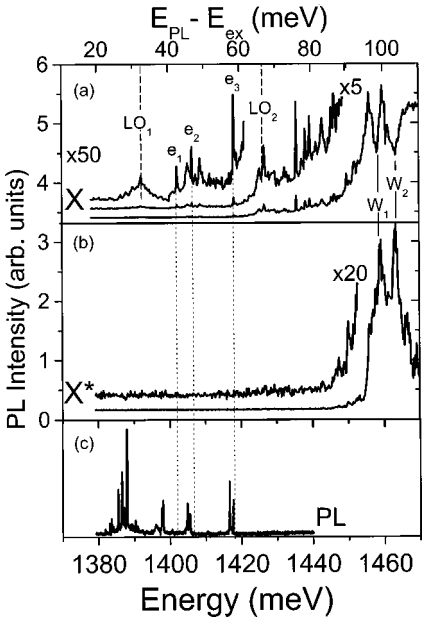

FIG. 4. PLE spectra from dot-B detecting on X (a) and X^* (b). Strong anticorrelation between the X and X^* PLE is seen in the region of the wetting layer transition at 1450 meV. At lower energies X^* is not excited, consistent with its attribution to a charged complex. For X, both sharp electronic resonances (e_1-e_3) and broader phonon-related features (LO_1,LO_2) are observed. (c) High power ($P_{ex}\sim100$ W cm^{-2}, $E_{ex}=1950$ meV) PL spectrum for direct comparison with PLE spectra.

rial, while X can be formed from resonant or nonresonant excitation.

The overall X,$2X$ versus P_e variations of Fig. 3(a) are well-fitted by rate-equation modeling[21] similar to the techniques of Refs. 18 and 19. The results are shown by the full curves in Fig. 3(a), good fits being obtained for both the X and $2X$ variations, further substantiating the $2X$ interpretation. As is physically reasonable, the power at which the single exciton (X and X^*) lines peak in intensity corresponds to a good approximation to an average exciton occupancy of one, independent of assumptions about the relative lifetimes of the exciton states occupied, thus allowing the horizontal axis in Fig. 3 to be interpreted in terms of average occupancy $\tilde{N}_X$ ($\tilde{N}_X=1$ from the fitting is labeled).[22] For $3X_s$, a greater than 2 power law is found ($m_{3X_s}=2.3\pm0.1$). This indicates that for $\tilde{N}_X>2$, the carrier capture rate into the dot is reduced and three-exciton occupation requires generation of more than three e-h pairs outside the dot per carrier capture-radiative cycle.

In order to obtain further information on the origin of X and X^*, PLE spectroscopy was performed. Figure 4 shows such spectra (dot-B), detecting on X [$E_{det}=1360.0$ meV, Fig. 4(a)] and X^* [$E_{det}=1361.5$ meV, Fig. 4(b)], respectively. For direct comparison, the excited-state PL spectrum, obtained for $\tilde{N}_X\gg2$, is plotted in Fig. 4(c). All PLE results were obtained using a laser excitation power such that the time-averaged exciton occupancy was $\tilde{N}_X\leqslant1$ over the range of excitation energy investigated. In the high-energy range of the spectra, both Figs. 4(a) and 4(b) exhibit broad yet structured features at ~1460 meV, corresponding to absorption into the wetting layer. Most importantly, the substructure shows a clear anticorrelation between X and X^* detection (peaks for X^* detection labeled $W_{1/2}$ correspond to dips in X, and vice versa). This anticorrelated behavior shows directly that X and X^* *compete* for photogenerated carriers, an observation consistent with both features arising from the same dot.

As E_{ex} is tuned to lower energy in Fig. 4(b), leading to direct excitation into the dot states ($E_{ex}<1450$ meV), X^* is no longer observed, independent of the excitation intensity used. It can thus be concluded that the formation of X^* relies on the photocreation of excitons/carriers outside the dot, within the body of the submicron mesa. In this case, separate electron-hole capture into the dot can occur and charged excitonic species consisting of unequal numbers of electrons and holes may be formed. By contrast, resonant excitation into the dot results in equal numbers of electrons and holes and the formation of charged excitons is extremely unlikely, since it requires the escape of one charge carrier. The single-exciton-like intensity dependence of X^*, combined with the absence of PLE for direct excitation of the dot, thus provides strong evidence that it arises from recombination of a charged single exciton.

The form of the PLE spectrum for X in Fig. 4(a) contrasts strongly with that for X^*. As the excitation energy is reduced below the wetting layer (WL) at 1450 meV, a continuum like[23] tail is observed in the spectrum extending ~40 meV below the WL transition. In addition, a number of sharp resonances are observed over the range 40–80 meV above the detection energy, similar to those reported in Refs. 23 and 24. These features [labeled e_1, e_2, and e_3 in Fig. 4(a)]

correlate well with the few-exciton features observed in the PL spectrum of Fig. 4(c). We thus identify these features as arising from absorption into single-exciton states of the dot, the negative energy shifts (~2–3 meV) between emission and absorption arising from the effects of Coulomb correlations. In addition to the sharp resonances, much broader features are observed close to $\Delta E = +31 \pm 2$ meV (LO_1) and $+63 \pm 3$ meV (LO_2), respectively. The larger linewidth of these features together with the relative energy at which they arise identify $LO_{n=1,2}$ as arising from phonon-assisted excitation of X involving n optical phonons. A more detailed account of the PLE spectra will be presented elsewhere.

The double heterostructure design of the structure allows further information on the X and X^* formation to be obtained, by tuning the excitation energy (E_{ex}) above the band gap of the $Al_{0.13}Ga_{0.87}As$ barrier material [$\sim 1690 \pm 5$ meV, dashed line in Fig. 1(a)]. This leads to global excitation of the samples, increasing the mesa-surface–absorption-volume ratio relative to 1520 meV excitation by a factor of ~8, and is expected to enhance the prevalence of charged species. Figure 2(b) compares the PL spectra obtained in the low power excitation limit $\tilde{N}_X < 1$ for such global ($E_{ex} = 1730$ meV) and local ($E_{ex} = 1520$ meV) excitation of dot-*A*. For global excitation, we find that X^* appears *before* X, in contrast with the result for local excitation of the mesa, supporting the above association between the appearance of charged species and the possibility for charging of the mesa surface, and hence for the attribution of X^* to a charged single-exciton complex.

It is difficult to ascribe X^* definitively to X^+ or X^-, i.e., X plus an excess hole (h) or an excess electron (e). However, the recent work of Refs. 16 and 17, in which X^- states were observed to lower energy than X in dots containing excess electrons, suggests that the charged complexes seen in our work, observed to higher energy than X, are more likely to arise from X^+, consistent with the expected larger h-h Coulomb repulsion than for e-e.[25] We also wish to comment that although our observation of charged excitons is in a mesa structure as employed by some other workers,[15] such charged complexes are also likely to arise in unprocessed material due to background residual charge in the material.

In summary, we have applied PL and PLE spectroscopy to the study of individual self-assembled In(Ga)As quantum dots. Emission was observed simultaneously from both charged and neutral single-exciton complexes. Combining PLE spectroscopy with detailed power-dependent measurements, we have identified the origin of the emission lines.

This work has been supported by EPSRC via Grant No. GR/L28828 and No. L78017.

[1] For a review see, e.g., *Quantum Dot Heterostructures*, edited by D. Bimberg, M. Grundmann, and N. N. Ledentsov (Wiley, Chichester, 1998).
[2] See, e.g., J. J. Finley, M. Skalitz, M. Arzberger, A. Zrenner, G. Böhm, and G. Abstreiter, Appl. Phys. Lett. **73**, 2618 (1998).
[3] P. Hawrylak, Phys. Rev. B **60**, 5597 (1999).
[4] U. Hohenester, F. Rossi, and E. Molinari, Solid State Commun. **111**, 187 (1999).
[5] Ph. Lelong and G. Bastard, Solid State Commun. **98**, 819 (1996).
[6] M. Barenco and M. A. Dupertuis, Phys. Rev. B **52**, 2766 (1995).
[7] G. Narvaez and P. Hawrylak, Phys. Rev. B **61**, 13 753 (2000).
[8] R. J. Warburton, C. S. Dürr, K. Karrai, J. P. Kotthaus, G. Medeiros-Ribeiro, and P. M. Petroff, Phys. Rev. Lett. **79**, 5282 (1997).
[9] K. H. Schmidt, G. Medeiros-Ribeiro, and P. M. Petroff, Phys. Rev. B **58**, 3597 (1998).
[10] E. Dekel, D. Gershoni, E. Ehrenfreund, D. Spektor, J. M. Garcia, and P. M. Petroff, Phys. Rev. Lett. **80**, 4991 (1998).
[11] F. Findeis, A. Zrenner, G. Böhm, and G. Abstreiter, Solid State Commun. **114**, 227 (2000).
[12] L. Landin *et al.*, Science **280**, 262 (1998); Phys. Rev. B **60**, 16 640 (1999).
[13] E. Dekel, D. Gershoni, E. Ehrenfreund, J. M. Garcia, and P. M. Petroff, Phys. Rev. B **61**, 11 009 (2000).
[14] A. Kuther, M. Bayer, A. Forchel, A. Gorbunov, V. B. Timofeev, F. Schäfler, and J. P. Reithmaier, Phys. Rev. B **58**, R7508 (1998).
[15] M. Bayer, O. Stern, P. Hawrylak, S. Fafard, and A. Forchel, Nature (London) **405**, 923 (2000).
[16] A. Hartmann, Y. Ducommun, E. Kapon, U. Hohenester, and E. Molinari, Phys. Rev. Lett. **84**, 5648 (2000).
[17] R. J. Warburton, C. Schäflein, F. Haft, F. Bickel, A. Lorke, K. Karrai, J. M. Garcia, W. Schönfeld, and P. M. Petroff, Nature (London) **405**, 926 (2000).
[18] M. Grundmann and D. Bimberg, Phys. Rev. B **55**, 9740 (1997).
[19] E. Dekel, D. Gershoni, E. Ehrenfreund, D. Spektor, J. M. Garcia, and P. M. Petroff, Phys. Rev. B **61**, 11 009 (2000).
[20] S. Malik, C. Roberts, R. Murray, and M. Pate, Appl. Phys. Lett. **71**, 1987 (1997).
[21] Our fitting involves the solution of coupled rate equations for the X,$2X$ and six higher-order complexes. For the X,$2X$ fitting, the important input parameters are the ratio of the radiative rates of X and $2X$, taken to be $r_X / r_{2X} = 0.5$, and their relative formation rates, taken to be $f_X / f_{2X} = 2$.
[22] The occupancy derived from the maxima of X and X^* in Fig. 3 agrees to within one order of magnitude with that calculated from the incident power and a radiative lifetime of 1 nsec. Considering uncertainties in the true active area of the mesa, this agreement is considered to be very fair.
[23] Y. Toda, O. Moriwaki, M. Nishioka, and Y. Arakawa, Phys. Rev. Lett. **82**, 4114 (1999).
[24] F. Findeis, A. Zrenner, G. Böhm, and G. Abstreiter, Solid State Commun. **114**, 227 (2000); A. Zrenner, M. Markmann, A. Paassen, A. L. Efros, M. Bichler, W. Wegscheider, G. Böhm, and G. Abstreiter, Physica B **256-258**, 300 (1998).
[25] R. J. Warburton, B. T. Miller, C. S. Durr, K. Karrai, J. P. Kotthaus, G. Medeiros-Ribeiro, P. M. Petroff, and S. Huant, Phys. Rev. B **58**, 16 221 (1998).